Dynamical (e,2e) Studies of Bio-Molecules

Joseph Douglas Builth-Williams

Submitted in ful lment for the requirements
of the degree of Masters of Science

March 2013

School of Chemical and Physical Sciences
Flinders University of South Australia

Science, like life, feeds on its own decay. New facts burst old rules; then newly divined conceptions bind old and new together into a reconciling law.

∼ William James (1842-1910)

6

Systematic Investigation of Three Structurally Related Cyclic Ethers

6.1 Introduction

Ethers are a type of organic compound defined as having an oxygen atom connected to two alkyl or aryl groups. Due to the oxygen atom with its two pairs of unbonded electrons, ethers are usually polar in nature which makes them useful for a number of purposes, including acting as solvents. Cyclic ethers, a type of heterocycle, are a class of ethers that are distinguished by their ring-like nature (See Figure 6.1).

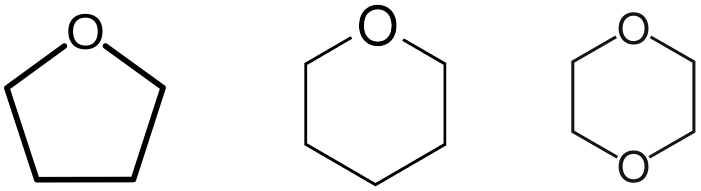

Tetrahydrofuran **Tetrahydropyran** **1,4-dioxane**

Figure 6.1: *Schematic diagram showing the structures of the three cyclic ethers.*

Tetrahydrofuran (THF), tetrahydropyran (THP) and 1,4-dioxane are three structurally similar cyclic ethers, as can clearly be seen in Figure 6.1. THF is a five membered ring, while THP and 1,4-dioxane are six membered rings. THF and THP both have a single oxygen atom located at the first position on their rings, while 1,4-dioxane has two oxygen atoms located at the first and fourth positions. The similar molecular structure of the three molecules also means that they share similar chemical properties, such as being low viscosity colourless liquids at room temperature.

THF is one of the most polar of all the ethers, so it finds great use as a solvent. It has a vapour pressure of 129 torr at 293°K, a melting point of 165°K and a boiling point of 339°K. THF's molecular formula is C_4H_8O, and it has a molar mass of 72.11 $gmol^{-1}$. THPs molecular formula is $C_5H_{10}O$, and it has a molar mass of 86.13 $gmol^{-1}$. In addition THP has a vapour-pressure of 40 torr at 293°K, a melting point of 228°K and a boiling point of 361°K. 1,4-dioxane is much like THP in having a six membered ring with an oxygen atom at the first position. It differs in that it also contains an oxygen atom at the fourth position on the ring (see Figure 6.1). 1,4-dioxane's molecular formula is $C_4H_8O_2$ and it has a molar mass of 88.11 $gmol^{-1}$. Its vapour-pressure is 30 torr at 293°K, its melting point is 284.95°K while its boiling point is 374.25°K.

All three of these organic molecules have been the subject of important previous studies. THF in particular is noteworthy as it has already been the subject of a dynamical (e,2e) study performed by Colyer *et al.* [36]. This particular study focused upon the HOMO orbital of THF, at scattered electron angles of -5°, -10° and -15°. The difference between the study previously performed by Colyer *et al.* and the present, is that Colyer *et al.* measured 10eV ejected electrons while this investigation focuses on 20eV ejected electrons.

THF has been the subject of a number of other relevant studies as well, the earliest of which was performed by Le Page *et al.* [134]. In that study, Le Page *et al.* investigated the differences in electron spectroscopy between the gas and solid phases. They found that an observed resonance feature in gaseous THF (located at 8.5eV and corresponding to vibrational excitation of the C-H bonds) shifted approximately 1eV in the solid-state THF. These results were obtained using 1-30eV incident electrons and by measuring the electron-energy-loss spectra. Brenton *et al.* also studied solid-state THF, specifically looking at electron-induced production of aldehydes within the sample [135]. That study was performed by condensing a layer of THF onto a solid Kr substrate, and then undertaking high-resolution electron-energy-loss spectroscopy using 1-18eV incident electrons to catalyse the aldehyde production. They found that there was a maximised aldehyde production associated with electron resonances/transient anion states.

Zecca *et al.* measured the Total Cross Section (TCS) of THF with both electrons and positrons as probes at incident energies below 21eV [123]. Mozejko *et al.* performed similar measurements but only using electrons, with their measurements being made over a much greater energy range: 1-370eV [124]. Both

of these studies showed a broad shape resonance in the 6-8eV region of the electron TCS. The elastic SDCS of THF was first measured by Milosavljevic *et al.* in 2005 [116]. This study was performed in the 20-300eV incident electron range, and over a scattered electron angle range of 10°-110°. The purpose of those results was to try and stimulate some interest in THF, in the larger theoretical community. Colyer *et al.* subsequently published elastic SDCS, Integral Cross Sections (ICS) and Momentum Transfer Cross Sections (MTCS) on THF, in addition to the aforementioned dynamical (e,2e) results [119]. These measurements were conducted within the 6.5 - 50eV electron energy range, and an angular range of 10° to 130°. At 6.5eV a shape resonance was observed in the elastic channel, with a width of approximately 2eV. A good summary of THF results for TCS, SDCS, ICS and MTCS can be found in Baek *et al.* [136].

THF has also been the subject of a number of EMS studies, most of which focused upon puckering and torsion within its ring structure [137, 138]. Because of its ring-like structure, THF is able to undergo pseudo-rotation, which is an internal motion that involves an out-of-plane puckering that rotates around the ring [131]. There are three possible conformations of gaseous THF, that are produced by this pseudo-rotation, which fall into the C_1, C_2 and C_s point group symmetry categories. These three conformations are very close in energy, and experimental evidence indicates that both the C_2 and C_s conformers coexist at room temperature [138]. Yang *et al.* showed that it was the C_s conformer that is slightly more preferred (at a 55% to 45% split), by comparing simulated orbital momentum density probability distributions to those measured using EMS [137].

THP has had fewer relevant studies performed on it, compared to THF, and certainly, to the best of our knowledge, no dynamical (e,2e) studies. There have been, however, a few electron scattering studies performed on THP, such as the one undertaken by Newbury *et al.* in 1986 [139]. Newbury *et al.* used electron energy-loss spectroscopy to study the carbon k-shell of gaseous furan, pyrrole, THF, pyrrolidine, piperidine and THP. Their measurements were taken at scattered electron angles in the range 1°-2°, with a final scattered electron energy of 2.5keV, over the electron loss range of 530eV to 575eV. Newbury *et al.* observed a single intense and broad feature in the oxygen k-shell spectrum, which they attributed to the carbon-oxygen bond. Breed *et al.* studied the molecular structure of THP, using electron diffraction from THP vapour in 1979 [140]. By deriving a simplified general valence force field from previous vibrational spectroscopic data, they were able to determine that THP is dominated by the C_s conformer when in a gaseous state.

The total electron-scattering cross section for THP was measured by Szmytkowski and Ptasińska-Denga in 2011 [141]. These measurements were performed using 1-400eV incident electrons and the results were compared to similar experiments performed on THF [124] and THFA [126]. Szmytkowski and Ptasińska-Denga found that THF and THP, being homologues, had a very similar TCS, though THP has a greater magnitude overall. The comparison between THP and THFA likewise showed a similar TCS shape, of comparable magnitude, although THFA showed a distinctive "double-peak" structure with a local minimum at around 8eV.

1,4-dioxane has been the subject of an EMS study, which was performed by Yang *et al.* in 2006 [142]. These authors used 600eV incident electrons to investigate the BES of the valence orbitals of 1,4-dioxane, and measured the momentum distribution of the HOMO. Those results were compared to results from theoretical calculations performed using Hartree-Fock and density functional theory, which were found to be in good agreement. Chapman and Hester performed conformational analysis upon 1,4-dioxane in an effort to understand the various structural distortions that can occur [143]. From their studies, they proposed two different mechanisms for 1,4-dioxane ring inversion, and found that the predicted Gibbs Free Energy was consistent with available experimental results.

Zecca *et al.* also studied THP and 1,4-dioxane as recently as 2012 [144]. They, however, used positrons to systematically investigate the scattering behaviour of the cyclic ethers oxirane, THP and 1,4-dioxane. In their study, Zecca *et al.* focused on using low-energy positrons (0.2-50eV) to measure the TCS for positron scattering from the aforementioned cyclic ethers. These results were compared to electron TCSs for oxirane and THP, and the authors suggested that the magnitude of the positron and electron TCSs were converging to a common value in the 200-300eV incident impact energy range.

6.1.1 Significance of the Molecules

The significance of the three cyclic ethers, chosen for the present investigation, cannot be underestimated. All three bear similar structures to moieties that make up DNA. THF, in particular, can be clearly seen in the structure of the sugar-phosphate backbone that holds the bases of the DNA together. Now while THP and 1,4-dioxane are not found in DNA systems, they both share similarities with the pyrimidine and purine bases that both contain six-membered rings. By studying a relatively large number of six-member heterocyclic molecules, we also

increase the body of work that theoreticians may draw from in the development of better theoretical tools. Finally, the structurally similar ethers also allows us to see whether structural, as well as dynamical, information can be gleaned using the present (e,2e) configuration.

6.2 Binding Energy Spectra

As previously mentioned, the BES was initially measured in order to determine the particular energies that must be selected in order to perform the TDCS measurements. Figures 6.2, 6.3 and 6.4 show the complete BES for THF, THP and 1,4-dioxane, respectively. For all three molecular targets, the scattered electron analyser was held at -10°, while the ejected analyser was held at 75°. Likewise, the incident and ejected electron energies were held at 250eV and 20eV, respectively, while the scattered electron energy was scanned across a range of energies.

The instrumental binding energy resolution was estimated in each case to be 1.1eV (FWHM), based upon the width of the binding energy peak for the helium $1s$ orbital, and we reiterate that all were measured under the same kinematic conditions. The Gaussian widths, employed in our deconvolution of the BES, are a convolution of the instrumental energy resolution and the natural orbital shell-width (Γ). Natural line-widths were obtained from relevant PES data. However, as $\Delta E_{BE} >> \Gamma$, it was found that approximating the Gaussian width to the binding energy resolution held true for all the orbitals studied and was sufficient for the fitting software used. The results of our fits to the present BES are also shown in Figures 6.2, 6.3 and 6.4.

6.2.1 Binding Energy Spectrum of Tetrahydrofuran

Figure 6.2 presents the complete BES for THF, along with relevant orbital assignments, and as should be apparent, is fitted with a total of 7 Gaussians. The orbital assignments were based upon the previous THF BES data measured using this particular (e,2e) spectrometer, and published by Colyer *et al.* [15, 35]. The orbital assignments used by Colyer *et al.* were, in turn, based on the data published by Yang *et al.*, which were collected as part of their EMS study on THF [137]. The orbital assignments used by Colyer *et al.* were further compared to the Ultraviolet Photoelectron Spectroscopy (UPS) data collected by Yamauchi *et al.* [145].

A total of seven Gaussian functions of fixed width has been fitted to the measured BES data by our fitting software [109]. As THF has a complex orbital

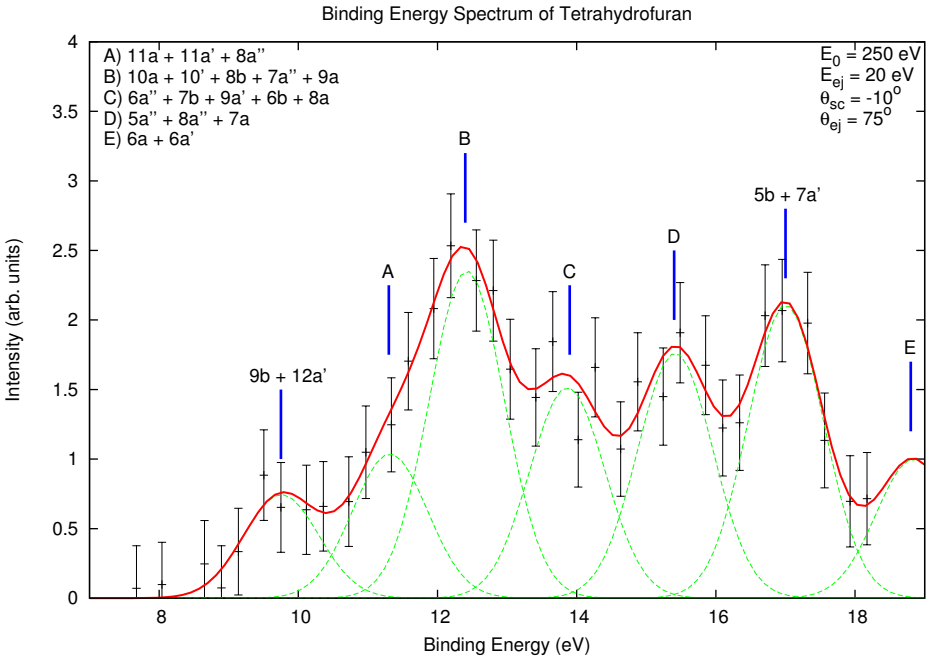

Figure 6.2: *The complete Binding Energy Spectrum of tetrahydrofuran in the range of* $7-19eV$. *See information on figure for further details. In should be noted here that the* $9b$ *and the* $12a'$ *orbitals are from different conformations (*C_2 *and* C_s*, respectively). See Table 6.1 for details on orbital assignments and their respective conformations.*

Table 6.1: *Ionisation potentials of THFA in eV, collected by Yang et al. [137], Yamauchi et al. [145], Giuliani et al. [146] and Colyer et al. [15, 35]. The "Present" column is data from the current work, and the theoretical calculations used were performed with the Outer Valance Green's Function (OVGF)/aug-ccp VDZ method.*

				Theory [146]			
Band	PES [137]	EMS [138]	UPS [145]	C_2	C_s	(e,2e) [15, 35]	Present
1	9.74	9.7	9.67	9.94 ($9b$)	9.91 ($12a'$)	9.7	9.75
2	11.52	12.14	11.41	11.65 ($11a$)	11.65 ($11a'$)	11.8	11.6
3			11.99	12.20 ($10a$)	11.89 ($8a''$)		
	12.52		12.48	12.43 ($8b$)	12.26 ($10a'$)	12.8	12.7
			12.90	12.62 ($9a$)	12.30 ($7a''$)		
4	14.1	14.54	14.00	14.21 ($7b$)	13.74 ($6a''$)	14.3	14.3
			14.45	14.82 ($6b$)	14.49 ($9a'$)		
5	15.4		15.29	14.95 ($8a$)	15.29 ($5a''$)		15.5
	16.8	16.74	16.70	16.57 ($7a$)	16.29 ($8a'$)	16.6	
6				16.93 ($5b$)	16.83 ($7a'$)	17.7	17.1
7	19.5	19.74	19.42	18.64 ($6a$)	18.67 ($6a'$)	19.6	18.8

structure, and the binding energy resolution is quite low, it is clear a number of orbitals are not well enough resolved to be given their own distinct peaks. Consequently the unresolved orbitals have been merged with the next closest orbital, and have been labelled as such. As discussed in Section 6.3, it should also be noted that the orbital assignments include orbitals for the two primary conformations of THF, C_2 and C_s. The HOMO of THF is a $9b$ orbital in the C_2 conformation and a $12a'$ orbital in the C_s conformation, and has thus been

labelled on Figure 6.2 as $9b + 12a'$. A table summarising the present BES data, the data collected by Colyer *et al.*, Yang *et al.*, and the UPS data reported by Yamauchi *et al.* is presented in Table 6.1.

6.2.2 Binding Energy Spectrum of Tetrahydropyran

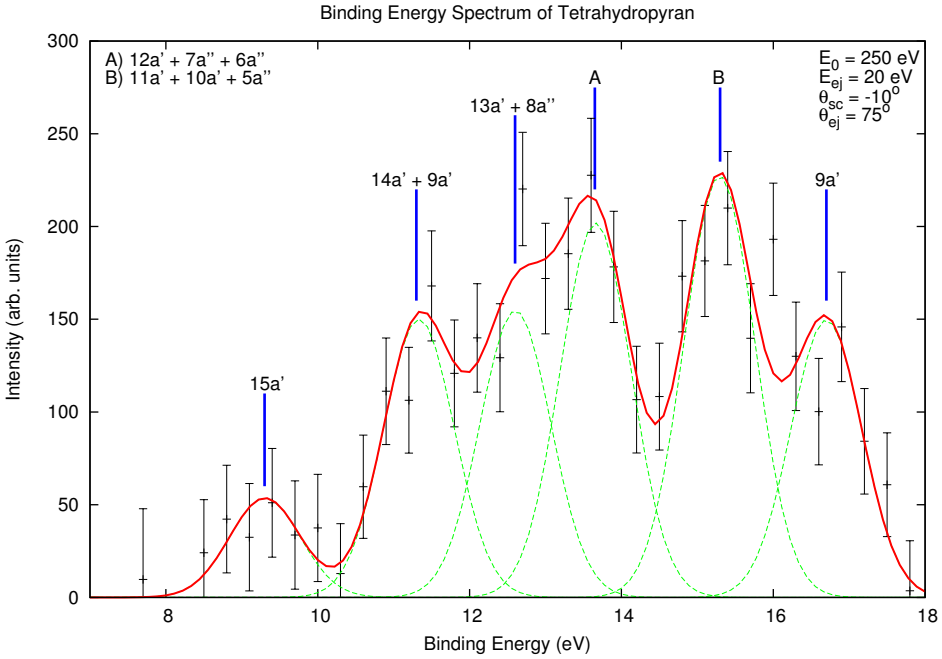

Figure 6.3: *The complete Binding Energy Spectrum of tetrahydropyran in the range of* $7 - 18eV$. *See information on figure for further details.*

The BES for THP can be seen in Figure 6.3, complete with its orbital assignments, and fitted with a total of 6 Gaussian functions. These orbital assignments were based upon the UPS data collected by Yamauchi *et al.* [145], as well as a calculation using the unrestricted Hartree-Fock (HF) method. A table summarising both the present BES data, as well as the UPS and unrestricted HF results, is presented in Table 6.2.

For the present THP BES, the experimental measurements were fitted with a total of six Gaussian functions, although twelve orbitals are predicted to exist in the binding energy range which was studied. Once again, the orbitals that were unable to be resolved from their neighbours were merged (combined) to their next closest neighbour. The HOMO for THP, which is the $15a'$ orbital, was for this species able to be completely resolved from the other molecular orbitals.

Table 6.2: *Ionisation potentials of THP (in eV) reported by Yamauchi et al. [145]. The "(e,2e)" column is data from the current work.*

Orbital	UPS [145]	Unrestricted HF [145]	(e,2e)
$15a'$	9.46	10.85	9.3
$14a'$	10.93	11.81	11.3
$9a''$	11.52	12.18	
$13a'$	12.10	13.09	12.6
$8a''$	12.50	13.42	
$12a'$	13.32	14.65	13.65
$7a''$	13.63	14.54	
$6a''$	14.25	15.76	
$11a'$	15.06	16.61	15.3
$10a'$	15.52	17.13	
$5a''$	15.90	17.18	
$9a'$	16.66	18.27	16.7
$8a'$	18.63	20.87	

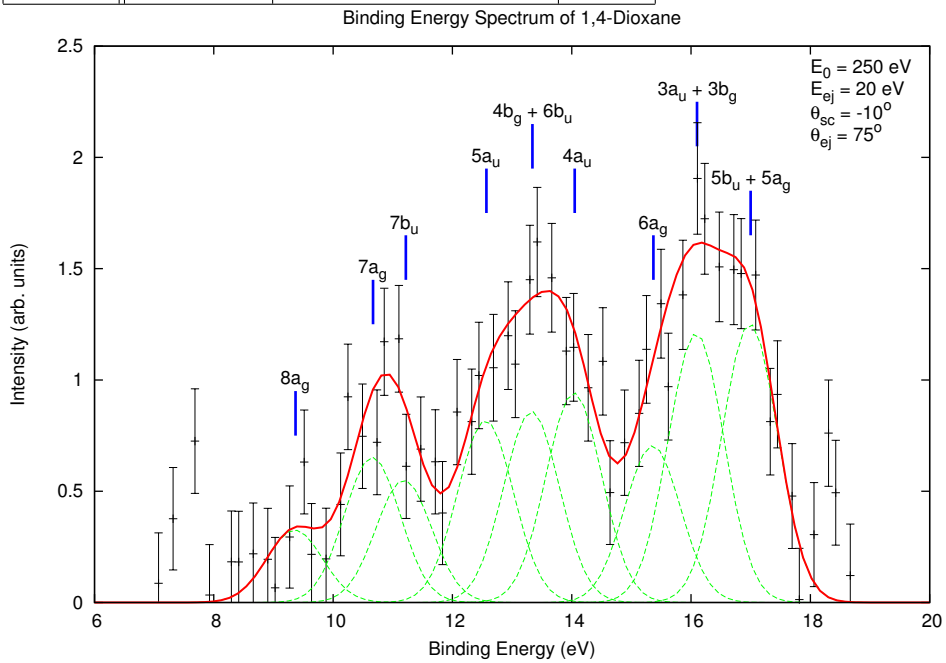

Figure 6.4: *The complete Binding Energy Spectrum of 1,4-dioxane in the range of* $7 - 19eV$. *See information on figure for further details.*

6.2.3 Binding Energy Spectrum of 1,4 - Dioxane

The 1,4-dioxane BES was given its orbital assignments based upon the UPS data and HF calculations provided by Yamauchi *et al.* [145]. Nine Gaussians were fitted to the present BES experimental data, however over the studied energy range 12 molecular orbitals are known to exist. As before, the unresolved orbitals were combined with that/those of their next closest Gaussian function. Unfortunately the $8a_g$ (HOMO) orbital of 1,4-dioxane was unable to be com-

pletely resolved from the NHOMO, suggesting that any TDCS measurements performed on it may also contain some contributions from the NHOMO.

Table 6.3: *Ionisation potentials of 1,4-dioxane (in eV) as reported by Yamauchi et al. [145]. The "(e,2e)" column is data from the current work.*

Orbital	UPS [145]	Unrestricted HF [145]	(e,2e)
$8a_g$	9.37	10.56	9.38
$7a_g$	10.67	12.08	10.68
$7b_u$	11.20	12.36	11.23
$5a_u$	12.57	14.03	12.58
$4b_g$	12.99	14.06	13.35
$6b_u$	13.34	14.64	
$4a_u$	14.05	15.21	14.06
$6a_g$	15.37	17.28	15.38
$3a_u$	16.1	17.35	16.2
$3b_g$	16.1	17.73	
$5b_u$	16.62	17.80	17.1
$5a_g$	17.00	18.96	
$4b_u$	19.33	21.76	

Figure 6.4 therefore shows the present BES for 1,4-dioxane, while Table 6.3 shows the molecular orbital assignments from this study, as well as the results provided by Yamauchi *et al.*. As before, a listing of the fitting data can be found in Appendix A (see Tables A.10, A.12 and A.14 for each of the relevant cyclic ethers), while a copy of the GNU Plot code can be found in Appendix B.

6.3 Specialised Experimental Considerations

All three cyclic ether samples (THF, THP and 1,4-dioxane) were purchased from Sigma-Aldrich, with a stated purity of 99%. However, as for pyrimidine and THFA, the samples were exposed to the air during their respective transfers to the sample vessel and thus may have picked up some minor contaminants. In order to maintain the purity of our samples, all three underwent three freeze-pump-thaw cycles, which has been previously discussed in Section 4.3.

Each of cyclic ethers studied are volatile liquids, which comes with its own particular set of problems. The most significant of these problems was the tendency for the ethers to condense within the gas capillary and on the inside of the chamber. These problems were overcome in the same fashion as they were for pyrimidine and THFA: by heating the capillary using THERMOCOAX and using heating strips to keep the chamber at a stable temperature of 40°C.

The final issue faced during the experiment, relevent only to THF, was which particular molecular conformation is dominant in the gaseous phase. As mentioned in Section 6.1, Yang *et al.* studied the gaseous phase of THF using EMS techniques and simulated orbital momentum density probability distributions [137]. The findings of Yang *et al.* showed that at room temperature the C_s conformation is preferred to the C_2 conformation by a ratio of 55% to 45%. As indicated by Table 6.1, the orbitals for the two conformers are very close in energy and as the energy resolution of our (e,2e) spectrometer is quite low, it is insufficient to resolve contributions from the two conformers. This meant that it would be almost impossible to differentiate them from one another, hence the BES and TDCS shows contributions from both conformers and the HOMO is assigned as being $9b + 12a'$.

6.4 Results and Discussion

Presented in this section are the theoretical and experimental TDCS results for the THF, THP and 1,4-dioxane molecules. For all three TDCSs the HOMO was probed with an intermediate incident electron energy of 250eV and an ejected electron energy of 20eV. All three were also measured at a sccattered electron angle of -5°, while the ejected electron analyser was moved in 5° steps and over an angular range of 65° to 120°, limited by the physical constraints imposed by the (e,2e) spectrometer components (see Section 3.1.4).

As the experimental TDCS measurements are relative in nature, they have in general been normalised to the M3DW calculations in order to give the best visual fit in the binary region, if possible. However as this is a comparative study of three cyclic ethers, the TDCS of all three were normalised at $\theta_b = 65°$ to the calculated value of the M3DW theory at that point. THF, due to its conformations, was normalised at $\theta_b = 65°$ to the calculated value of the combined $9b + 12a'$ M3DW theory, rather than the individual $9b$ or $12a'$ calculated values as discussed earlier and expanded upon more below. Tables of the experimental data listing the TDCSs for all three cyclic ethers, after normalisation, can be found in Appendix A, in Tables A.11, A.13 and A.15. Note that the value of θ_b used in the normalisation process is not crucial to the discussion that follows.

As can be seen in Figure 6.5, THF under the current kinematics has a rather broad binary peak. As Colyer *et al.* [36] noted, albeit with a slightly different kinematic setup, the recoil peak of THF was relatively large compared to the binary peak and this also holds true under our kinematic conditions. Furthermore, both the binary and recoil peaks are offset from the momentum transfer

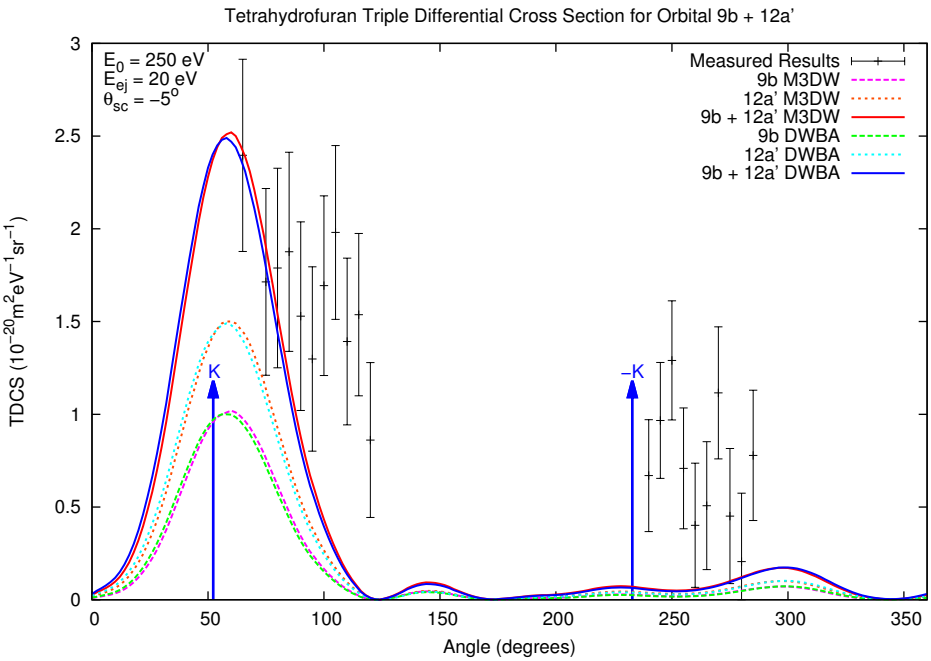

Figure 6.5: *TDCS of tetrahydrofuran, measured at the scattered electron angle of* $-5°$*, where* $E_0 = 250$ *eV and* $E_{ej} = 20$ *eV. The solid red line represents the combined M3DW results for* $9b + 12a'$*, while the solid blue line represents the combined DWBA results for* $9b + 12a'$*.*

direction ($\vec{\kappa}$ and $-\vec{\kappa}$), and in the case of the recoil peak, significantly so. The scatter in the data that comprise the recoil peak, is possibly due to the difficulty in measuring at such small scattered electron angles, as well as the somewhat lower count rates associated with the recoil peak.

Figure 6.5 also shows the results of a number of theoretical calculations performed by Madison and collegues, specifically DWBA and M3DW results, for the $9b$ and $12a'$ orbitals. Due to the aforementioned situation with the conformations of THF being a 45%-55% split, between the $12a'$ and $9b$ orbitals, the experimental results were normalised to the combination of both, with the appropriate weighting. Both sets of theoretical results predict a relatively narrow binary peak and a very small recoil peak. Neither of these predictions were supported by the experimental results and, in fact, the highly similar nature of the DWBA and M3DW results suggest that the additional PCI terms included in the M3DW calculations are having little effect on the calculated results under the present kinematics. This, as noted earlier in this thesis, seems a little paradoxical, given the shifts in the binary and recoil peaks from $+\vec{\kappa}$ and $-\vec{\kappa}$ which might suggest that PCI is a factor here.

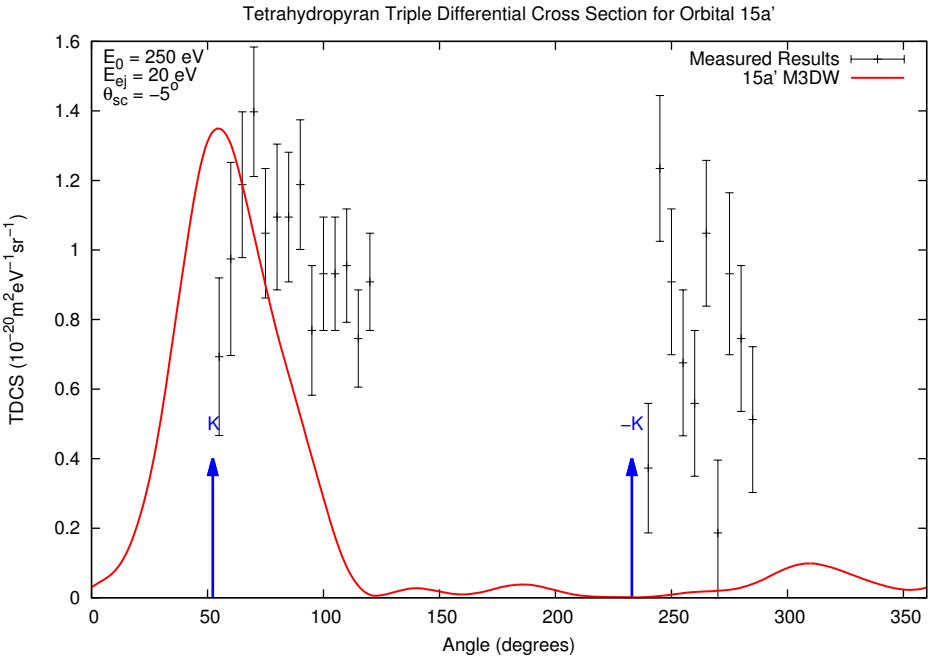

Figure 6.6: *TDCS of the* $15a'$ *orbital of tetrahydropyran, measured at the scattered electron angle of* $-5°$*, where* $E_0 = 250$ *eV and* $E_{ej} = 20$ *eV. The solid red line represents the M3DW results.*

Figure 6.6 presents the experimental and theoretical results for THP. The experimental binary peak is broad and the recoil peak is relatively large in magnitude. As with THF, the recoil peak at such a small scattered electron angle was a challange to measure, resulting in some amount of data scatter. Furthermore, rather unusually from our experience with the TDCS presented as a part of this thesis, the measured binary peak to recoil peak ratio was close to unity.

Unlike the THF results described earlier, only one set of calculations was performed for THP. Those M3DW results can be seen for the $15a'$ (HOMO) orbital in Figure 6.6. These M3DW results predict a narrow binary peak and a very small recoil peak. While neither of these predictions have been observed experimentally, the agreement between theory and experiment for THP is better than that for THF in the binary region. However the observed recoil peak magnitude is almost entirely counter to that from the prediction, even if we allow for the scatter in the measured results and the quite large error-bars.

The results for 1,4-dioxane are presented in Figure 6.7, along with the theoretical results of a M3DW calculation performed by Madison and colleagues. As with the other cyclic ethers already discussed, 1,4-dioxane has a broad binary peak and a relatively large recoil peak (compared to the binary peak).

However, unlike the previous cyclic ethers, there is little scatter in the TDCS recoil peak, and a well defined and quite narrow peak structure is observed. Also observed is a distinct shift of the observed binary and recoil peaks away from the momentum transfer direction, which is particularly prominent in the recoil region.

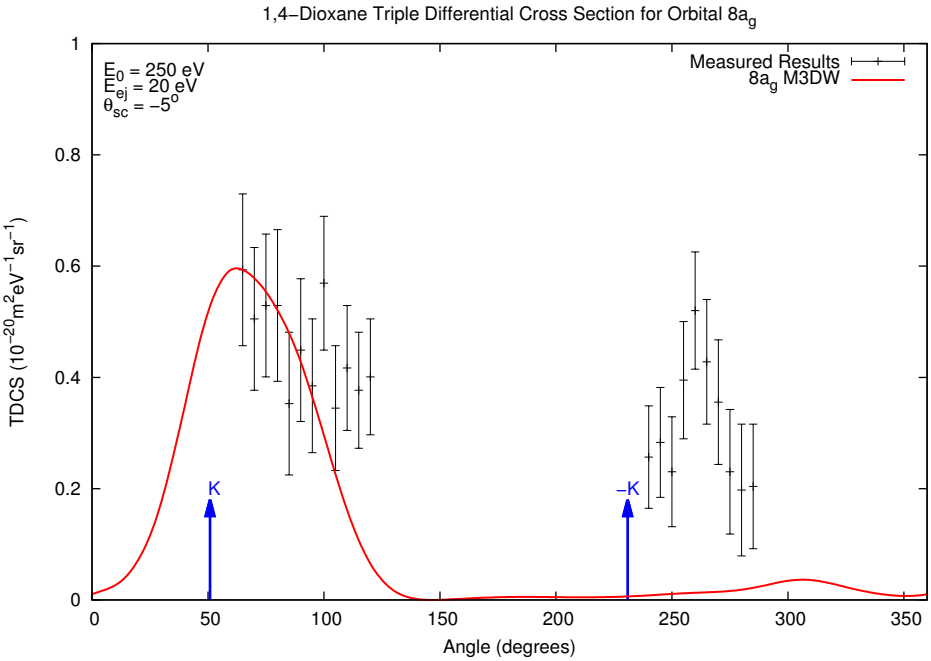

Figure 6.7: *TDCS of the* $8a_g$ *orbital of1,4-Dioxane, measured at the scattered electron angle of* $-5°$*, where* $E_0 = 250$ *eV and* $E_{ej} = 20$ *eV. The solid red line represents the M3DW results.*

The M3DW results for the $8a_g$ orbital are also displayed in Figure 6.7 as a solid red line. Those results reproduce the measured binary peak quite well, successfully predicting 1,4-dioxanes broad peak under these kinematic conditions. However, as seems to be the trend, it again fails to predict the magnitude or position of the recoil peak. This once more is evidence for the current theoretical model underestimating the electron-electron and/or electron-residual ion correlations and their effect upon the observed TDCS. Such an underestimation might be due to the nuclear charge in the calculations being spread over a spherical shell which is, of course, unphysical and an artefact of this method.

Comparing the three sets of experimental and theoretical results (see Figure 6.8) together leads to some interesting observations. However, before elucidating those observations, it should be noted once again about the relative nature of the experimental results, and how they are normalised to the theory TDCS

result at $\theta_{ej} = 65°$. It should further be noted that the binary peak to recoil peak ratio was taken at $\theta_{ej} = 85°$ and 265°, respectively, in all sets of measurements so that a comparison might reasonably be drawn (see Table 6.4). Finally, the observed magnitude of the M3DW results for THF should be viewed in the context of the TDCS being the weighted sum of the two HOMO orbitals for the two conformations of THF.

Table 6.4: *The current binary to recoil peak (B-R) ratios found in the present study for the cyclic ethers THF, THP and 1,4-dioxane.*

Cyclic ether	B-R ratio	Error
Tetrahydrofuran	2.001	±0.713
Tetrahydropyran	1.072	±0.404
1,4-dioxane	1.218	±0.537

With that last point in mind, it is interesting to note the magnitude differences between the three cyclic ethers. Specifically, we observe a trend towards smaller binary peak magnitudes as the mass of the molecule under consideration increases. However the recoil peak magnitude for the three cyclic ethers seems to have the inverse relationship, namely the larger molecular masses lead to a relatively larger recoil peak. Please note that this conclusion is somewhat less definitive, due to the size of the uncertainties on the TDCS in the recoil peak which occur as these are very difficult experiments. Shape-wise, all three cyclic ethers display a rather broad binary peak with a similarly broad recoil peak, with perhaps the exception to this latter observation being 1,4-dioxane. Furthermore, all three molecules display binary and recoil peaks that are displaced from the momentum transfer directions $+\vec{\kappa}$ and $-\vec{\kappa}$, respectively. This suggests that PCI effects might be playing an important role in the scattering dynamics in each system.

It is also interesting to compare the M3DW results between the three cyclic ethers. For THF and THP there is little observed difference between the TDCS at their binary peaks, given the addition of a carbon atom to the molecular structure. However there is a slight but noticeable shift in θ_{ej} for a secondary peak in the 200°-250° angular region in THF to the 150°-200° angular region of THP. On the other hand, the small recoil peak at ∼300° in THF is now slightly shifted to greater angles in THP. 1,4-dioxane, however, displays no secondary peak features and instead has a recoil peak with a smaller magnitude at around the same location in θ_{ej} as that for THP. 1,4-dioxane is also different in having a rather broad binary peak predicted by the theory, rather than the narrower binary peaks predicted for THF and THP. We speculate that this may reflect

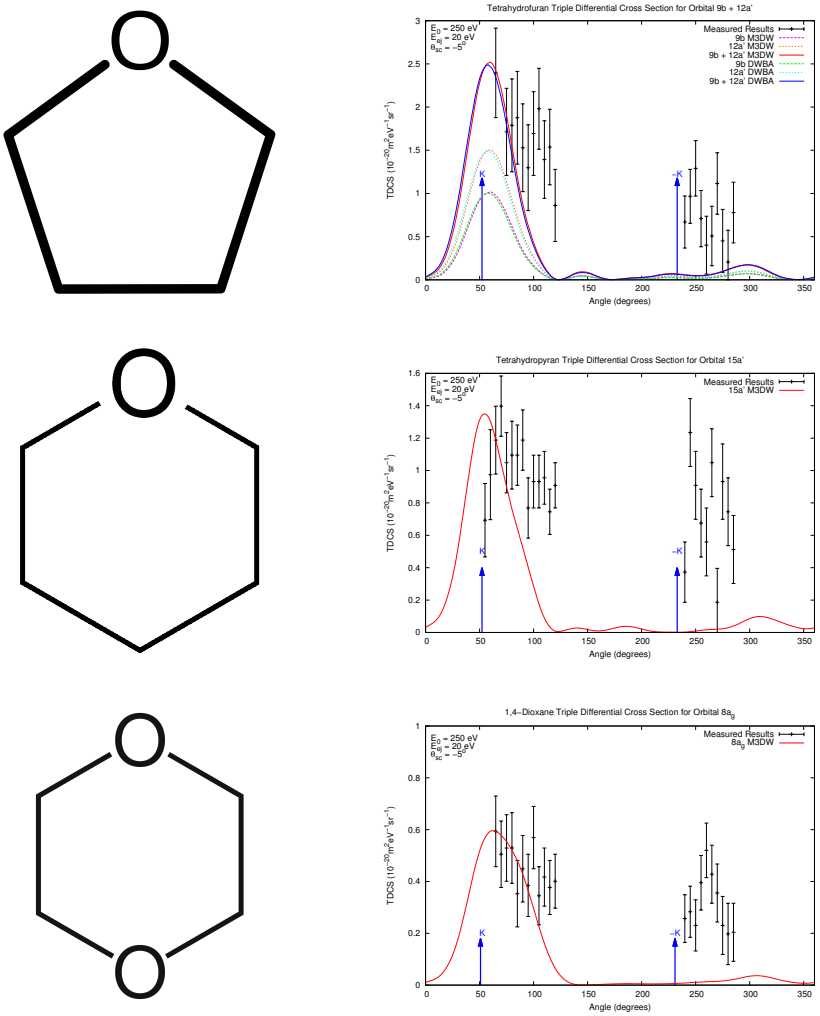

Figure 6.8: *Summary diagram showing all the present TDCSs for the HOMOs of THF, THP and 1,4-dioxane (as labelled) and the corresponding M3DW theoretical results. See the legends in each panel for further details.*

the additional lone electon pairs on 1,4-dioxane, compared to THF and THP.

Finally, as with all the biomolecules studied within this thesis, the recoil peak size predicted by the M3DW is far exceeded by the observed recoil peak magnitude. At the time of writing and as canvassed earlier, two alternative explanations for this have been put forward by Colyer *et al.* [15] and Xu *et al* [114]. Colyer *et al.* suggested that the observed discrepancy is due to the lack of nuclear charge at the molecules in question centre-of-mass [15]. Xu *et al.* suggested, however, that this observation was due to the specific symmetry of the orbital being probed at the kinematical conditions under consideration [114].

6.5 Conclusion

In this chapter experimental and theoretical dynamical (e,2e) results were presented for three structurally similar cyclic ethers. There have been previous studies on these three cyclic ethers, ranging from electron-scattering experiments [116, 119, 134, 135, 139, 140] and including total cross sections [123, 124, 141], EMS studies [137, 138, 142] and for THF even a previous dynamical (e,2e) experiment [36]. However, the present investigation represents the first dynamical (e,2e) measurements performed under the current kinematic conditions on THF, THP and 1,4-dioxane. Notwithstanding that point, the measured binding energies and orbital assignments for the present binding energy spectra were found to be in good agreement with the previous (e,2e) and UPS studies.

The current TDCS measurements were performed using 250eV incident electrons and 20eV ejected electrons, at the scattered electron angle of -5°. For all three cyclic ethers, the HOMO was studied which equates to the $15a'$ and $8a_g$ orbitals for THP and 1,4-dioxane, respectively. The HOMO for THF was also studied, but due to the 45%-55% split of the two primary conformations the TDCS results are a weighted sum of the $9b$ and $12a'$ orbitals. Furthermore, all three cyclic ethers were normalised to the results of M3DW calculations at $\theta_{ej} = 65°$ and the binary peak to recoil peak ratio was calculated in each case by measuring at $\theta_{ej} = 85°$ and 265°, respectively.

All three cyclic ether TDCSs displayed a relatively broad binary peak and a recoil peak that was relatively large in comparison to the binary peak. Additionally, the scatter observed in some of the experimental TDCS results were thought to be due to the difficulty in measuring the low-intensity HOMO of the cyclic ethers at small scattered electron angles.

Overall, the M3DW calculations were found to have had mixed levels of success in reproducing the experimental data: while the M3DW calculations totally failed to predict the recoil peak magnitudes, the M3DW calculations did have some success with predicting the shape of the binary peak. In particular, the M3DW model showed great promise in predicting the shape of the binary peak of 1,4-dioxane, while it performed in a less successful manner with regards the the shape of the binary peaks of THF and THP. Further work and development into the M3DW model is clearly necessary, although it should be noted that a new method of calculating the M3DW is in its preliminary stages of use and has shown great promise in terms of reproducing the available experimental results for CH_4 [78].

Finally, we had originally hoped that by studying three structurally related molecules that we might also extract some information pertaining to their molecular structures as well as the dynamics of the scattering process in each case. In this regard we were hindered by the difficulty of the experiments when concentrating on the HOMO, leading to somewhat larger error bars (as noted above). Nonetheless, some of the differences observed in the TDCS for THF compared to THP compared to 1,4-dioxane might be ascribed to the different structural features of those species.